

## Self-assembly of cubic colloidal particles at fluid-fluid interfaces by hexapolar capillary interactions

### SUPPLEMENTARY INFORMATION

Giuseppe Soligno,<sup>1</sup> Marjolein Dijkstra,<sup>2</sup> and René van Roij<sup>1</sup>

<sup>1</sup>*Institute for Theoretical Physics, Center for Extreme Matter and Emergent Phenomena,  
 Utrecht University, Princetonplein 5, 3584 CC Utrecht, The Netherlands*

<sup>2</sup>*Soft Condensed Matter, Debye Institute for Nanomaterials Science, Department of Physics,  
 Utrecht University, Princetonplein 1, Utrecht 3584 CC, The Netherlands*

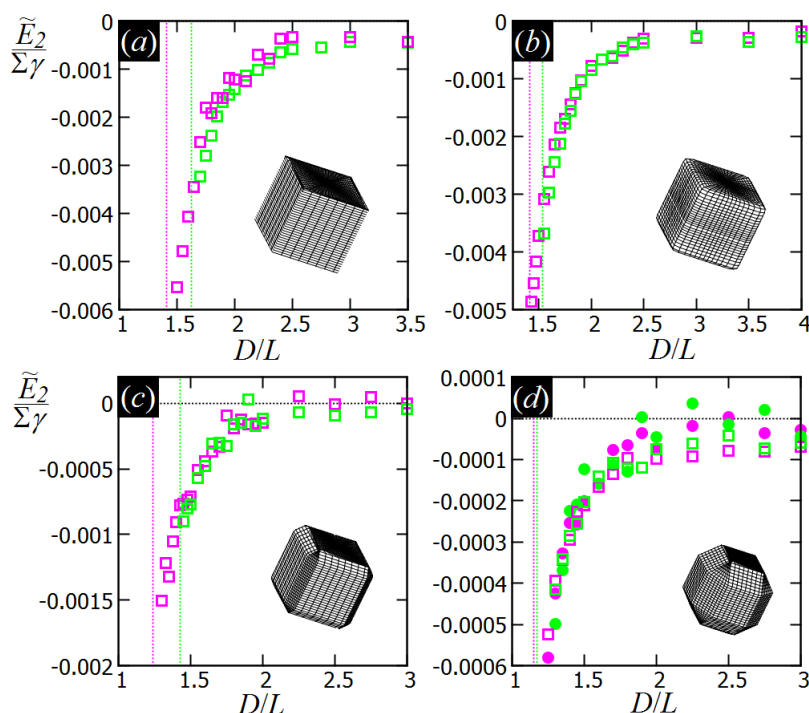


Figure S1: Interaction energy  $\tilde{E}_2$  [Eq. (3)] for two adsorbed particles at a center of mass distance  $D = \sqrt{(x_1 - x_2)^2 + (y_1 - y_2)^2}$ , with  $\varphi_i, \psi_i, z_i$  (see Fig. 1), for  $i = 1, 2$ , given by their equilibrium value found in Sec. III A, and with azimuthal orientation  $\alpha_i$  such that the particles are dipole-dipole interacting (pink symbols) and tripole-tripole interacting (green symbols). The energy is plotted in units of  $\Sigma\gamma$ , with  $\Sigma$  the total surface area of one particle and  $\gamma$  the fluid-fluid surface tension. A sketch of the dipole-dipole and tripole-tripole bonds is shown in Fig. 4(a) – (c). The particle shape considered is (a) a sharp-edge cube, (b) a smooth-edge cube, (c) a slightly truncated-edge cube, and (d) a highly-truncated edge cube. For the highly truncated-edge cube, the hexapolar deformation is not 3-fold symmetric like for the other three particle shapes, as one depression and one rise in the interface height profile are slightly more spread and less intense than the remaining two rises and two depressions (that is two of the six poles of the hexapole have a different magnitude than the other four, see the contour plots in Fig. 3). In (d), we show with pink squares the dipole-dipole bond between two dipoles both with two poles of the same magnitude, and with pink disks the dipole-dipole bond between two dipoles both with two poles of different magnitude. Analogously, we show with green squares the tripole-tripole bond between two tripoles both with the less intense pole of the hexapole as the central pole of the tripole, and with green disks the tripole-tripole bond between two tripoles both with the less intense pole of the hexapole as a lateral pole of the tripole. As shown, the behavior of  $\tilde{E}_2(D)$  for the highly truncated-edge cube is similar in all these cases, proving that the non-exactly-3-fold symmetry of its hexapolar capillary deformation does not affect significantly the results.

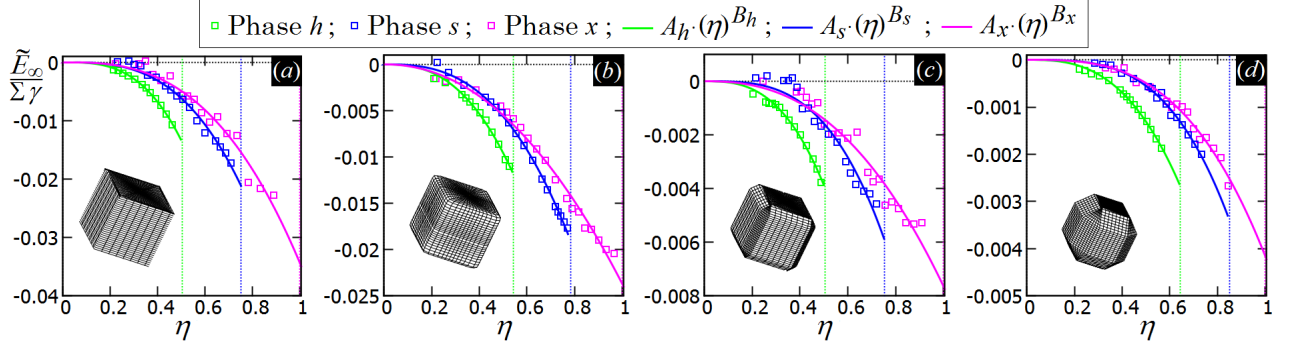


Figure S2: (Capillary) interaction energy per particle  $\tilde{E}_\infty$  [Eq. (3)], as computed through our numerical method, for 2D periodic lattices of particles adsorbed at a fluid-fluid interface, with each particle generating a hexapolar capillary deformation (see Fig. 3). The energy is plotted in units of  $\Sigma\gamma$ , with  $\Sigma$  the total surface area of one particle and  $\gamma$  the fluid-fluid surface tension. Green refers to a honeycomb lattice [phase  $h$ , see Fig. 4(d),(e)], blue to a square lattice [phase  $s$ , see Fig. 4(f)], and pink to a hexagonal lattice [phase  $x$ , see Fig. 4(g)]. The particle shape is (a) a sharp-edge cube, (b) a smooth-edge cube, (c) a slightly truncated-edge cube, and (d) a highly-truncated edge cube (see exact definitions of these particle shapes in Appendix A). In the graphs, the squares are the results from our numerical simulations, obtained for various particle densities, i.e. using different sizes of the lattice unit cell. The particle density  $\eta$  is normalized such that  $\eta = 1$  for the close-packed hexagonal lattice. The full lines represent a fit of our numerical data, for the phases  $h$ ,  $s$ ,  $x$ , with  $A_\alpha \cdot (\eta)^{B_\alpha}$ , where  $A_\alpha$  and  $B_\alpha$  are the fit parameters (with  $\alpha = h, s, x$ , respectively) and their obtained values is reported in Tab. S1. The vertical dotted lines indicate the close-packed density, i.e. when the particles are at their contact distance, for the honeycomb lattice (phase  $h$ , in green), for the square lattice (phase  $s$ , in blue), and for the hexagonal lattice (phase  $x$ , in pink).

	$A_h/(\Sigma\gamma)$	$B_h$	$A_s/(\Sigma\gamma)$	$B_s$	$A_x/(\Sigma\gamma)$	$B_x$
(a)	-0.1100	3.0364	-0.0502	3.0242	-0.0344	2.8081
(b)	-0.0584	2.6087	-0.0371	2.7209	-0.0237	2.1091
(c)	-0.0274	2.8213	-0.0132	3.0052	-0.0076	2.4411
(d)	-0.0093	2.8307	-0.0059	3.4183	-0.0042	3.0774

Table S1: With respect to the results in Fig. S2, we show here the values of the fit parameters  $A_\alpha$  and  $B_\alpha$  ( $\alpha = h, s, x$ ), obtained by fitting  $\tilde{E}_\infty(\eta)$  with  $A_\alpha (\eta)^{B_\alpha}$ , for the particle lattice phases  $h$ ,  $s$ ,  $x$ , and for (a) sharp-edge cubes, (b) smooth-edge cubes, (c) slightly truncated-edge cubes, and (d) highly-truncated edge cubes. The subscripts  $h$ ,  $s$ , and  $x$  indicates the particle phase in which  $\tilde{E}_\infty(\eta)$  was computed.

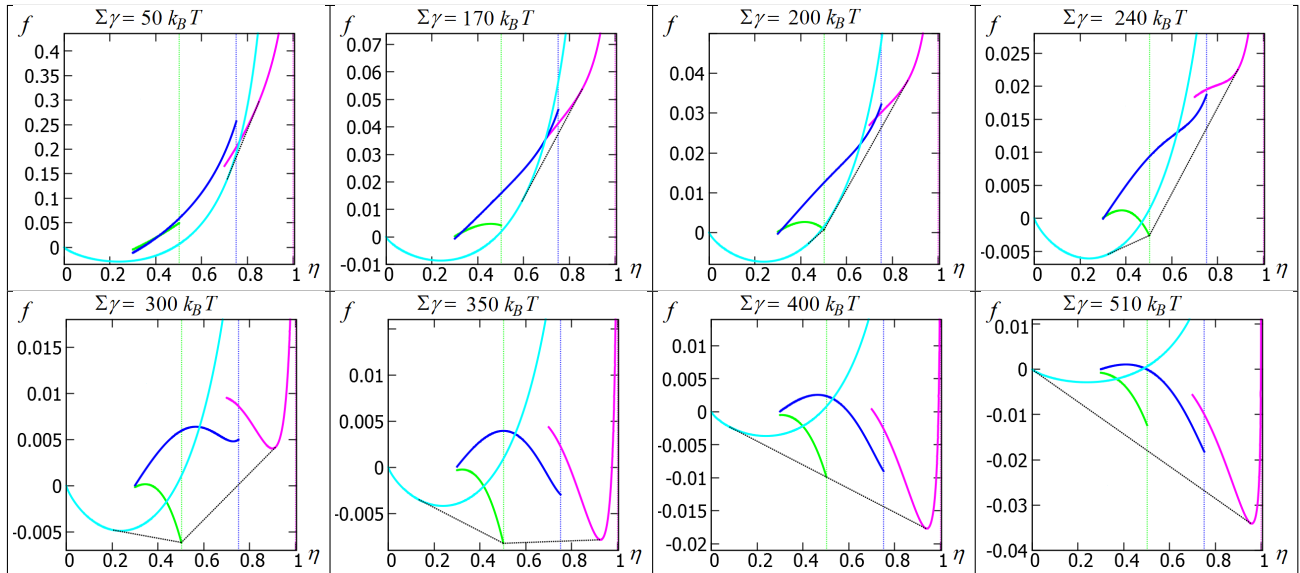


Figure S3: For sharp-edge cubes, plots of  $f(\eta, T)$  [Eq. (6)] for the phase  $f$  (light-blue),  $h$  (green),  $s$  (blue), and  $x$  (pink) with respect to the normalized density  $\eta$  (with  $\eta = 1$  for the close-packed phase  $x$ ), for some values of  $\Sigma\gamma/k_B T$  (with  $\gamma$  the fluid-fluid surface tension,  $\Sigma$  the total surface area of the particle,  $k_B$  the Boltzmann constant and  $T$  the temperature). The dotted vertical lines represents the close-packing values of  $\eta$  for the phases  $h$  (green),  $s$  (blue),  $x$  (pink). The common tangent constructions [70] (black dotted lines) indicate where phase coexistence occur.

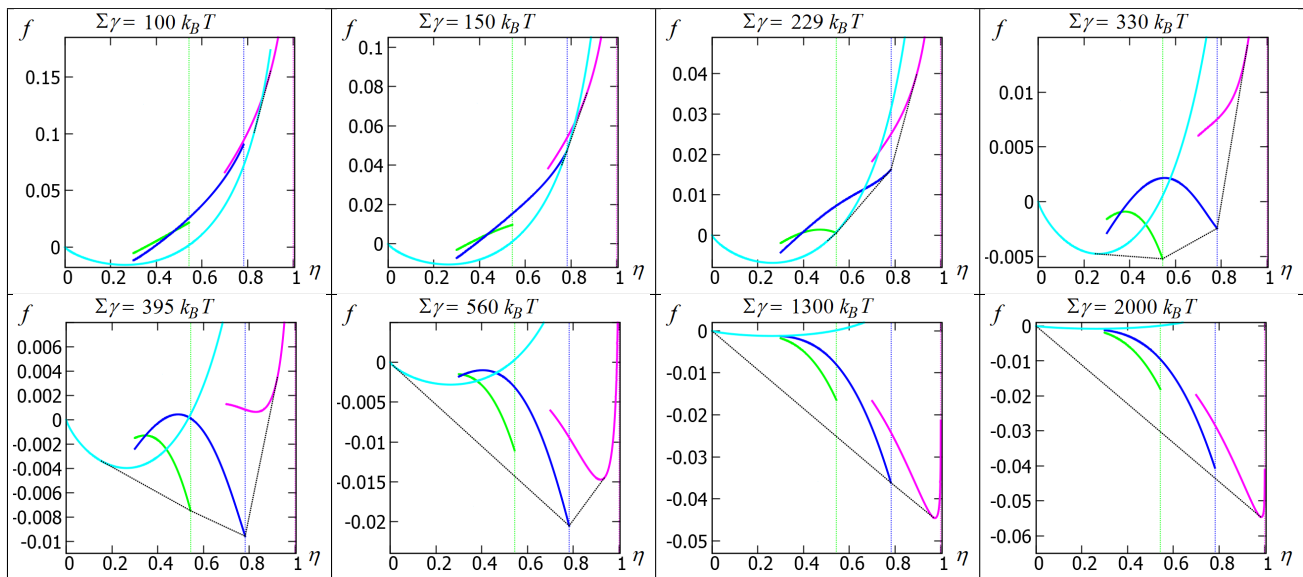


Figure S4: For smooth-edge cubes, plots of  $f(\eta, T)$  [Eq. (6)] for the phase  $f$  (light-blue),  $h$  (green),  $s$  (blue), and  $x$  (pink) with respect to the normalized density  $\eta$  (with  $\eta = 1$  for the close-packed phase  $x$ ), for some values of  $\Sigma\gamma/k_B T$  (with  $\gamma$  the fluid-fluid surface tension,  $\Sigma$  the total surface area of the particle,  $k_B$  the Boltzmann constant and  $T$  the temperature). The dotted vertical lines represents the close-packing values of  $\eta$  for the phases  $h$  (green),  $s$  (blue),  $x$  (pink). The common tangent constructions [70] (black dotted lines) indicate where phase coexistence occur.

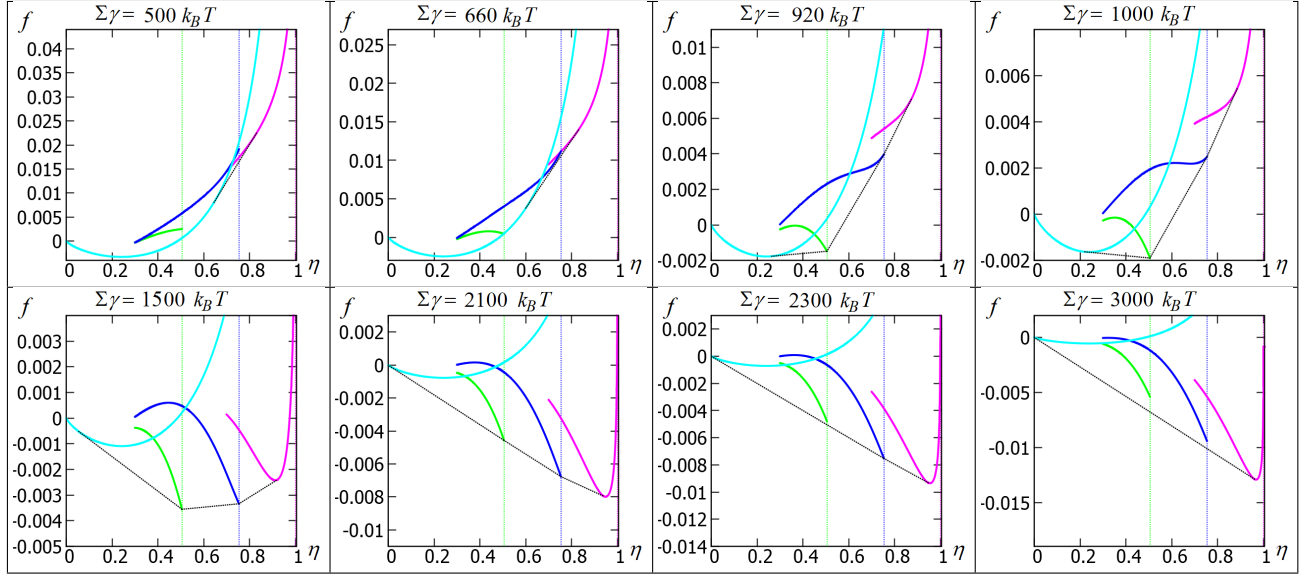


Figure S5: For slightly truncated-edge cubes, plots of  $f(\eta, T)$  [Eq. (6)] for the phase  $f$  (light-blue),  $h$  (green),  $s$  (blue), and  $x$  (pink) with respect to the normalized density  $\eta$  (with  $\eta = 1$  for the close-packed phase  $x$ ), for some values of  $\Sigma\gamma/k_B T$  (with  $\gamma$  the fluid-fluid surface tension,  $\Sigma$  the total surface area of the particle,  $k_B$  the Boltzmann constant and  $T$  the temperature). The dotted vertical lines represents the close-packing values of  $\eta$  for the phases  $h$  (green),  $s$  (blue),  $x$  (pink). The common tangent constructions [70] (black dotted lines) indicate where phase coexistence occur.

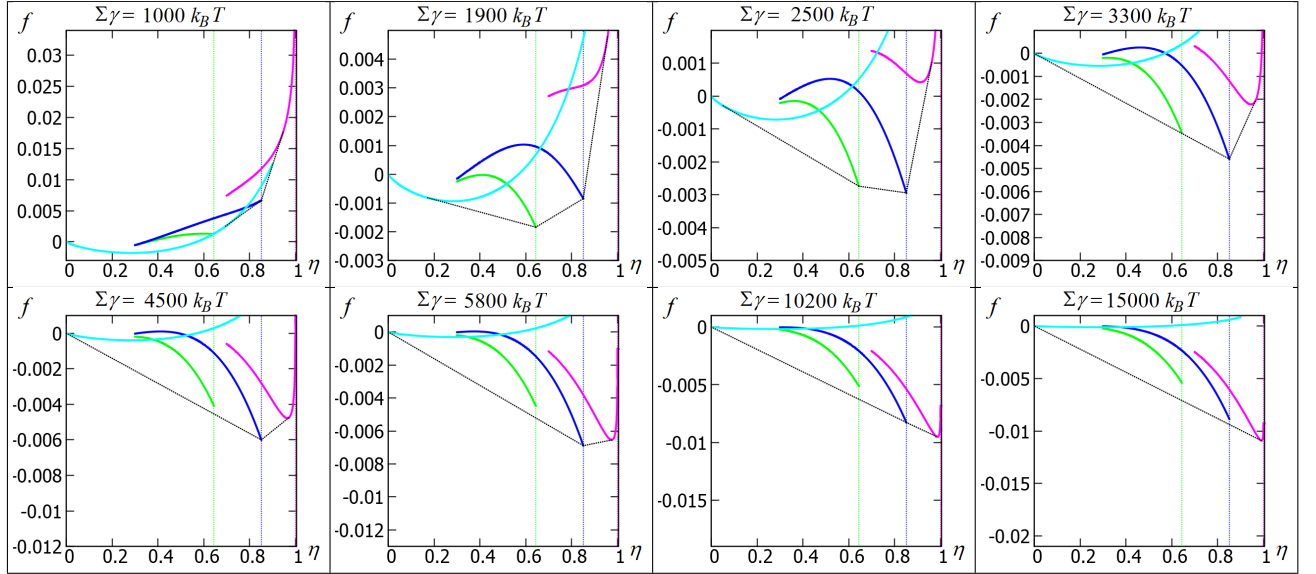


Figure S6: For highly truncated-edge cubes, plots of  $f(\eta, T)$  [Eq. (6)] for the phase  $f$  (light-blue),  $h$  (green),  $s$  (blue), and  $x$  (pink) with respect to the normalized density  $\eta$  (with  $\eta = 1$  for the close-packed phase  $x$ ), for some values of  $\Sigma\gamma/k_B T$  (with  $\gamma$  the fluid-fluid surface tension,  $\Sigma$  the total surface area of the particle,  $k_B$  the Boltzmann constant and  $T$  the temperature). The dotted vertical lines represents the close-packing values of  $\eta$  for the phases  $h$  (green),  $s$  (blue),  $x$  (pink). The common tangent constructions [70] (black dotted lines) indicate where phase coexistence occur.

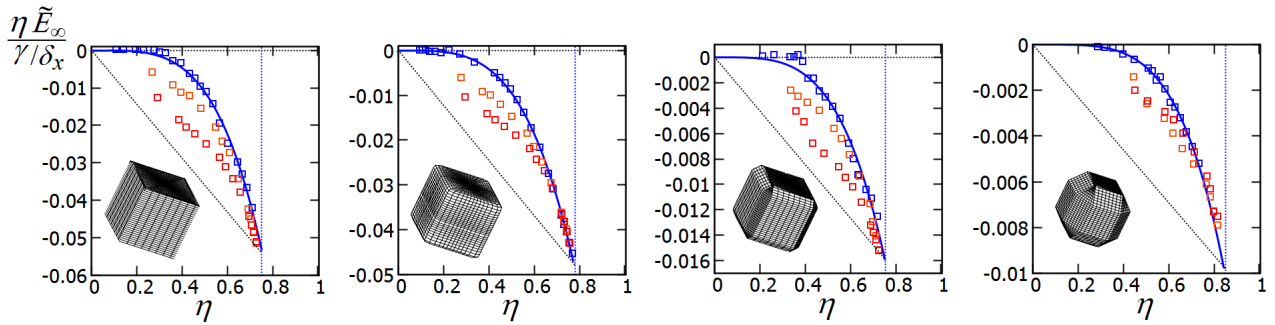


Figure S7: (Capillary) interaction energy per particle  $\tilde{E}_\infty$  [Eq. (3)] with respect to the normalized particle density  $\eta$  (where  $\eta = 1$  for the close-packed phase  $x$ ) for smooth-edge cubes in phase  $s$ , as obtained by our numerical method. Here  $\tilde{E}_\infty$  is multiplied by the particle density  $\eta$  and plotted in units of  $\gamma/\delta_x$ , with  $\delta_x$  the particle density of the close-packed phase  $x$  (see Tab. II) and  $\gamma$  the fluid-fluid surface tension. The blue vertical dotted line indicates the close-packed value of  $\eta$  for the phase  $s$ . The blue symbols are the results obtained using the unit cell of the phase  $s$  defined in Appendix C, Sec. B. The red and orange symbols indicate the results obtained using a rectangular unit cell for the phase  $s$ . Precisely, the orange points are simulations for cubes in phase  $s$  having contact distance in the tripole-tripole bond direction of the lattice, while the distance in the dipole-dipole bond direction of the lattice is fixed by the particle density, and the red points are simulations for cubes in the phase  $s$  having contact distance in the dipole-dipole bond direction of the lattice, while the distance in the tripole-tripole bond direction of the lattice is fixed by the particle density. From the common tangent construction [70], see black dotted line, it follows that at equilibrium the close-packed phase  $s$  coexists with an empty phase (i.e. a phase with  $\eta = 0$ ), for any density  $\eta$  of particles at the fluid-fluid interface. Since near the close-packed particle density the interaction energy  $\tilde{E}_\infty$  is the same for the different unit cells (as expected, since they all converge to the same unit cell at the close-packed density), it does not matter for our results if we use a square or rectangular unit cell for the phase  $s$ . In principle, the rectangular unit cells (red and orange symbols) are energetically more favorable than a square cell for lower particle densities, however such density regimes are excluded by the common tangent constructions, so it is irrelevant which unit cell we use. For the other particle shapes considered in the paper we expect qualitatively similar results.

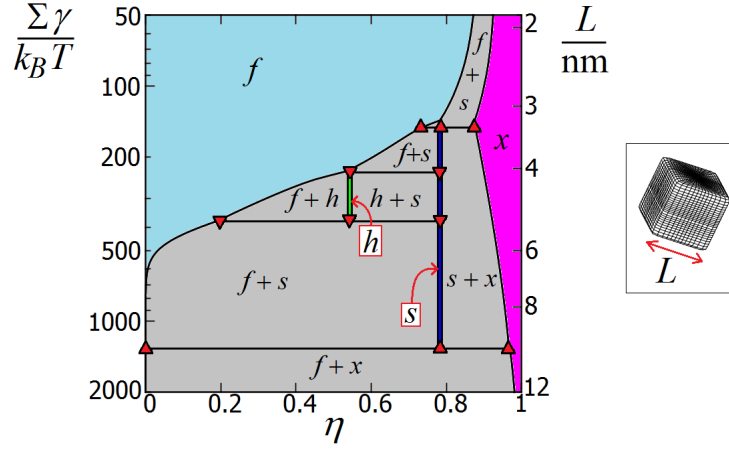
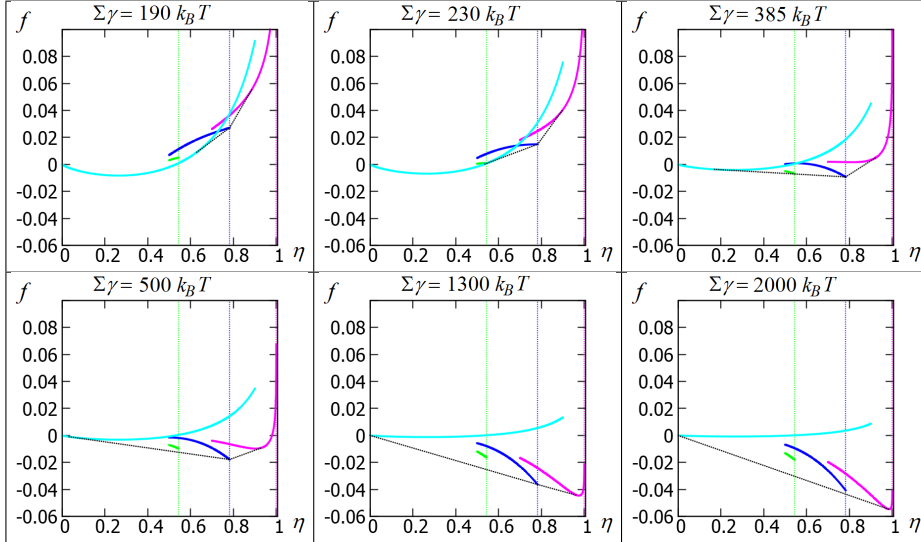


Figure S8: Temperature-density phase diagram for adsorbed smooth-edge cubes at a fluid-fluid interface. The left vertical axis is  $\gamma\Sigma/(k_B T)$ , with  $\gamma$  the fluid-fluid surface tension,  $\Sigma$  the total surface area of a particle,  $k_B$  the Boltzmann constant, and  $T$  the temperature (note that the low temperature or big particle limit is in the verse toward down of the vertical axis). The right vertical axis represents the corresponding value of the particle size  $L$  (see exact definition in Appendix A) at room temperature and using a typical surface tension  $\gamma = 0.01$  N/m. The horizontal axis is the particle density  $\eta$ , normalized such that  $\eta = 1$  for the close-packed  $x$  phase. The colored areas indicate where a pure phase exists on the whole fluid-fluid interface: light-blue for phase  $f$  (disordered phase), green for phase  $h$  (honeycomb lattice), blue for phase  $s$  (square lattice), and pink for phase  $x$  (hexagonal lattice). The gray areas indicate where coexistence between two phases occurs, and the red symbols mark the triple points where three phases coexist. The Young contact angle considered here is  $\pi/2$ , so the cubes are always adsorbed at the interface in the 111 configuration (i.e. with a vertex toward up, see Sec. III A). The results presented in this phase diagram are obtained by plotting  $f(\eta, T)$  [Eq. (6)] for the various particle phases  $f$ ,  $h$ ,  $s$ , and  $x$ , with respect to  $\eta$  and at different values of  $\Sigma\gamma/(k_B T)$ , and then by performing common tangent constructions [70]. Here we use the crystal hard disk free energy  $F_{xhd}$  [Eq. (19)] in the free energies of the phases  $h$  and  $x$  [Eqs. (15) and (16), respectively] to compute  $F_S$  in Eq. (6), while in the results of Fig. 6 we used the fluid hard disk free energy  $F_{fhd}$  [Eq. (18)]. However, the phase diagram obtained here is almost identical to the one shown in Fig. 6 for the smooth-edge cubes. This proves that our approximations in the estimation of the particle entropy by analytical hard-disk expressions are, as we expected, not very relevant. The reason is that we consider the interplay between capillary and hard-particle interactions in the regime where capillarity is the leading force, i.e.  $\Sigma\gamma \gg k_B T$ , hence a rough estimation of the hard-particle interactions is enough to accurately predict the self-assembly of the system. On the bottom, we show  $f(\eta, T)$  [Eq. (6)] for the phase  $f$  (light-blue),  $h$  (green),  $s$  (blue), and  $x$  (pink) for some values of  $\Sigma\gamma/k_B T$ , obtained using  $F_{xhd}$  [Eq. (19)] instead of  $F_{fhd}$  [Eq. (18)] in Eqs. (15) and (16). The dotted vertical lines represents the close-packing values of  $\eta$  for the phases  $h$  (green),  $s$  (blue),  $x$  (pink). The common tangent constructions [70] (black dotted lines) indicate where phase coexistence occur.



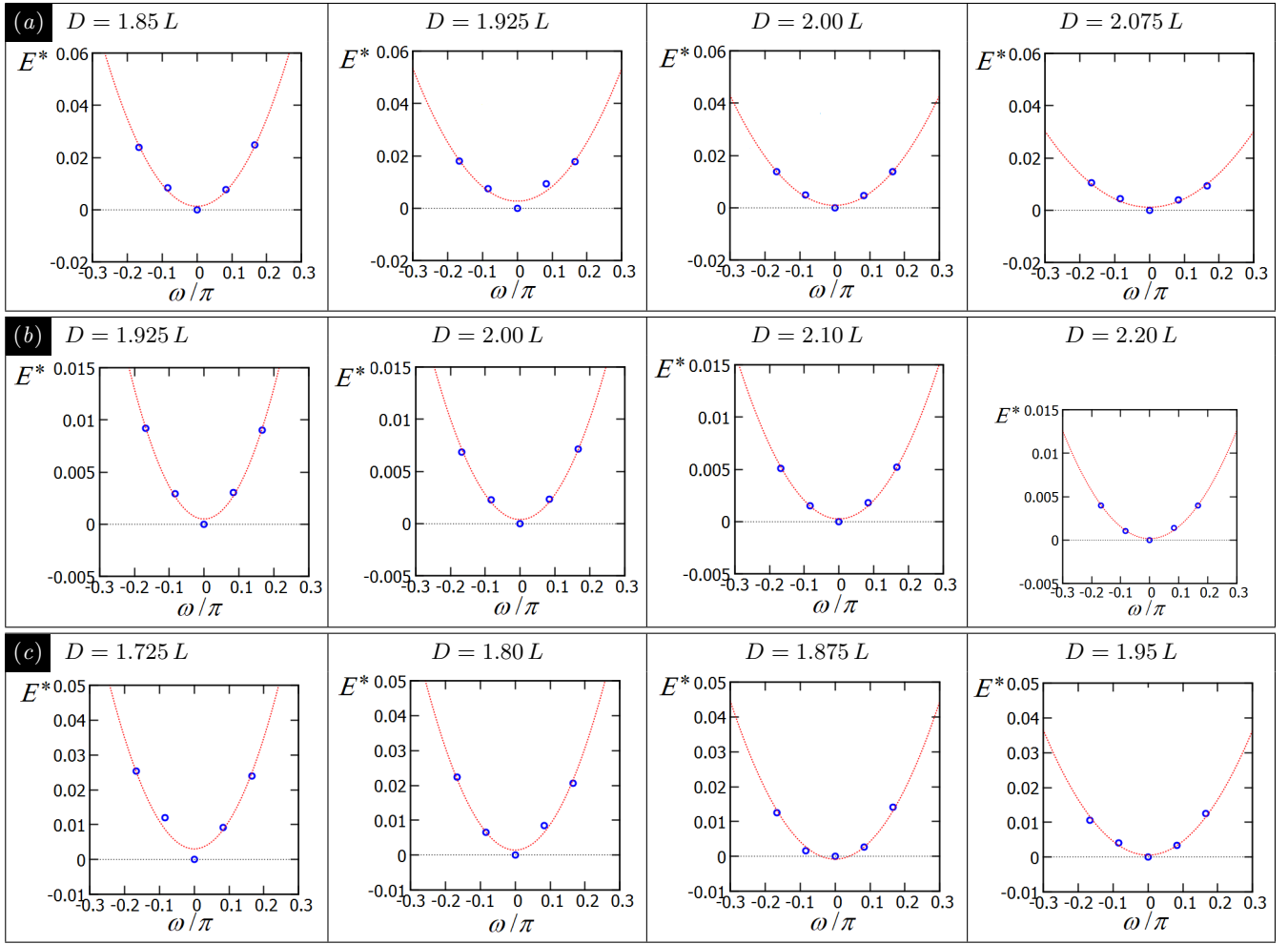


Figure S9: Energy  $E_N(\omega, \eta)$ , obtained through our numerical method and in units of  $\Sigma \gamma$  (with  $\gamma$  the fluid-fluid surface tension and  $\Sigma$  the particle surface area), for sharp-edge cubic particles at a fluid-fluid interface and in the lattice phase (a)  $x$ , (b)  $h$ , and (c)  $s$ , where  $\omega$  is the out-of-equilibrium azimuthal rotation we impose on one particle (for the exact definition of the particle configuration used here for each phase see Fig. 12). The blue symbols are  $E^* \equiv [E_N(\omega, \eta) - E_N(\omega = 0, \eta)]/(\Sigma \gamma)$  obtained for various particle-particle center-of-mass distances  $D$ , corresponding to different particle densities  $\eta$  (see Appendix C, Sec. B). The red dotted lines represent a fit of  $E_N(\omega, \eta) - E_N(\omega = 0, \eta)$  with  $U(\omega) \equiv C(\eta) \frac{\omega^2}{2}$ . The values of  $C(\eta)$  obtained from the fit for the various phases are shown in Fig. 12.

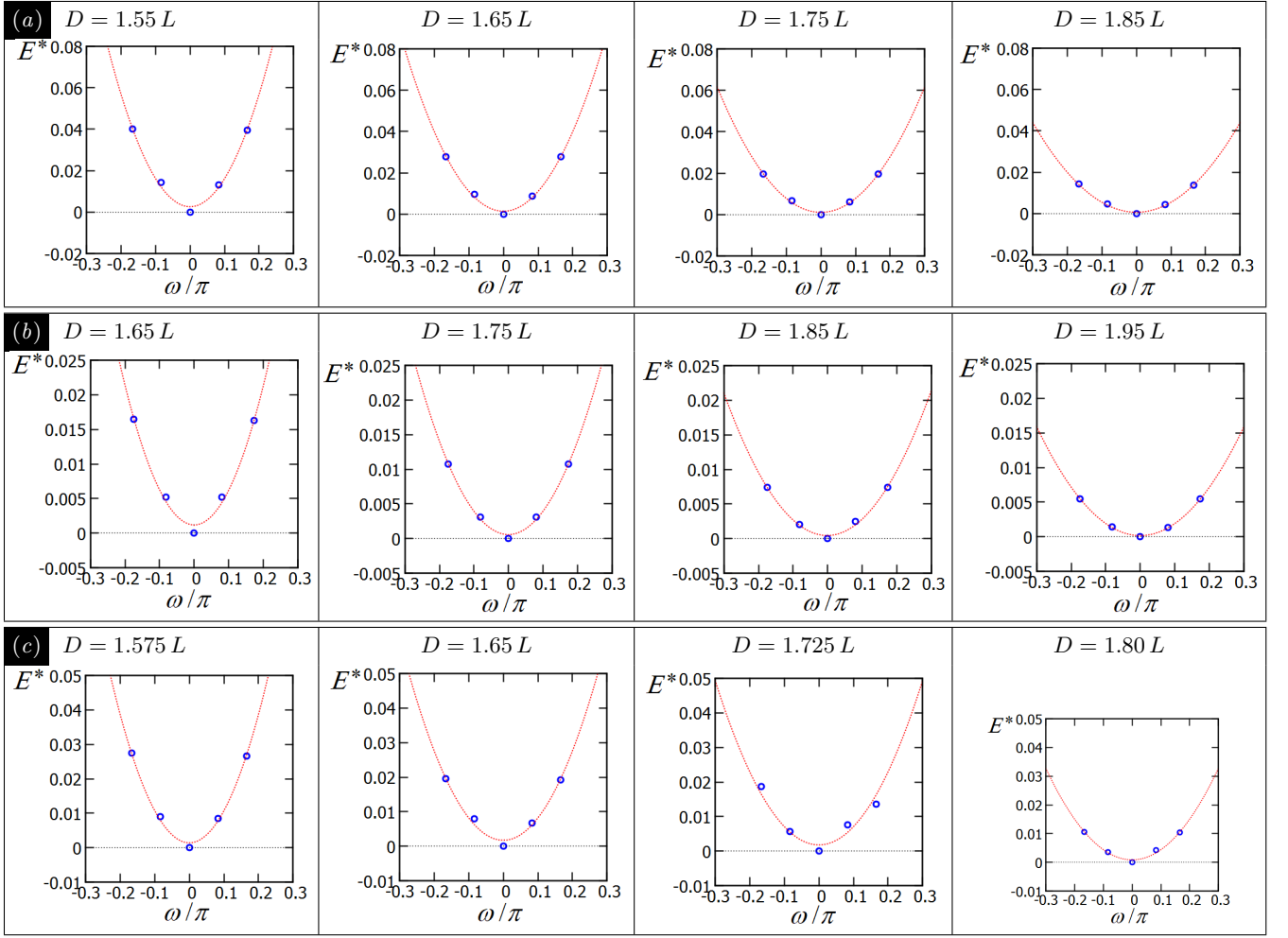


Figure S10: Energy  $E_N(\omega, \eta)$ , obtained through our numerical method and in units of  $\Sigma\gamma$  (with  $\gamma$  the fluid-fluid surface tension and  $\Sigma$  the particle surface area), for smooth-edge cubic particles at a fluid-fluid interface and in the lattice phase (a)  $x$ , (b)  $h$ , and (c)  $s$ , where  $\omega$  is the out-of-equilibrium azimuthal rotation we impose on one particle (for the exact definition of the particle configuration used here for each phase see Fig. 12). The blue symbols are  $E^* \equiv [E_N(\omega, \eta) - E_N(\omega = 0, \eta)]/(\Sigma\gamma)$  obtained for various particle-particle center-of-mass distances  $D$ , corresponding to different particle densities  $\eta$  (see Appendix C, Sec. B). The red dotted lines represent a fit of  $E_N(\omega, \eta) - E_N(\omega = 0, \eta)$  with  $U(\omega) \equiv C(\eta) \frac{\omega^2}{2}$ . The values of  $C(\eta)$  obtained from the fit for the various phases are shown in Fig. 12.

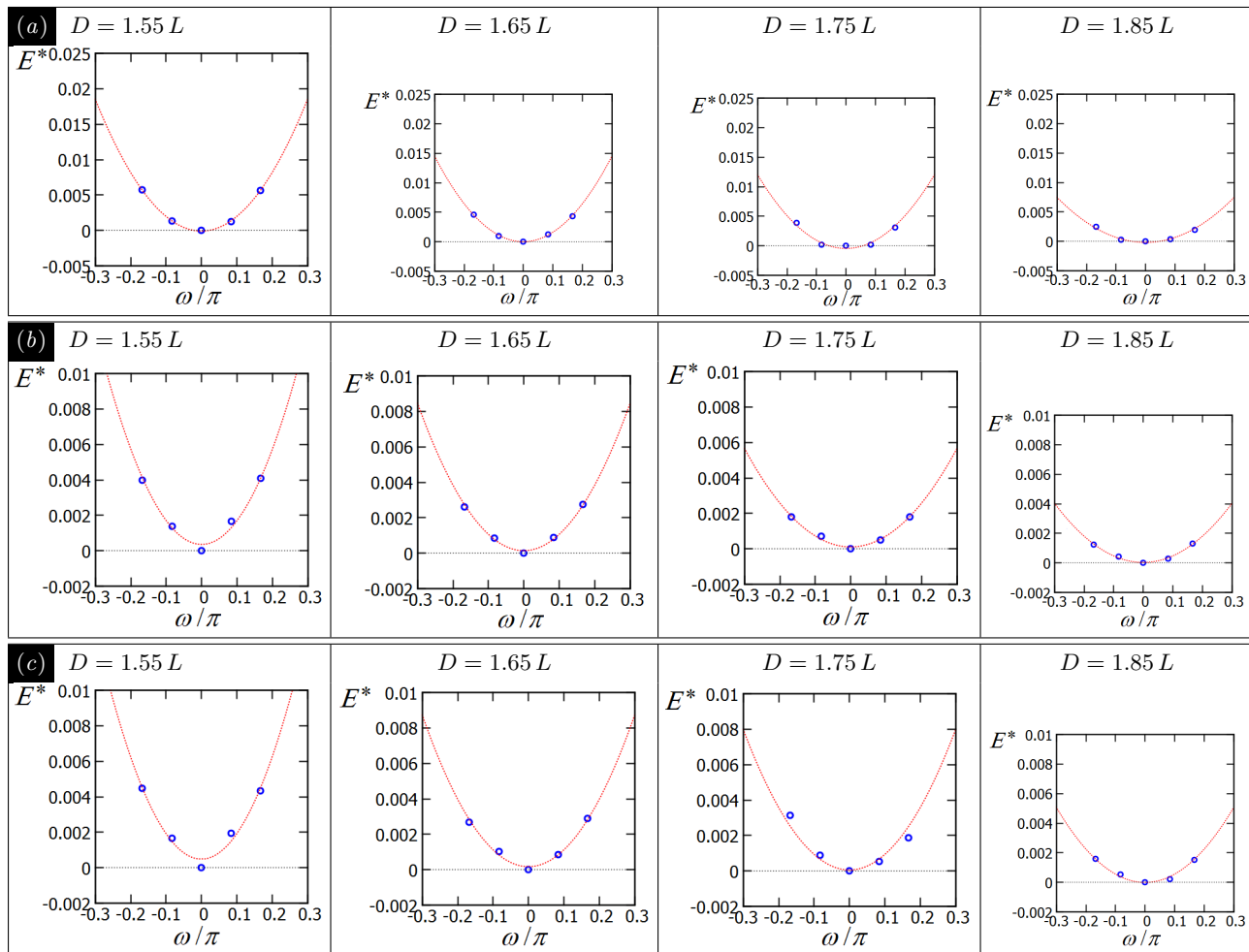


Figure S11: Energy  $E_N(\omega, \eta)$ , obtained through our numerical method and in units of  $\Sigma \gamma$  (with  $\gamma$  the fluid-fluid surface tension and  $\Sigma$  the particle surface area), for slightly truncated-edge cubic particles at a fluid-fluid interface and in the lattice phase (a)  $x$ , (b)  $h$ , and (c)  $s$ , where  $\omega$  is the out-of-equilibrium azimuthal rotation we impose on one particle (for the exact definition of the particle configuration used here for each phase see Fig. 12). The blue symbols are  $E^* \equiv [E_N(\omega, \eta) - E_N(\omega = 0, \eta)]/(\Sigma \gamma)$  obtained for various particle-particle center-of-mass distances  $D$ , corresponding to different particle densities  $\eta$  (see Appendix C, Sec. B). The red dotted lines represent a fit of  $E_N(\omega, \eta) - E_N(\omega = 0, \eta)$  with  $U(\omega) \equiv C(\eta) \frac{\omega^2}{2}$ . The values of  $C(\eta)$  obtained from the fit for the various phases are shown in Fig. 12.

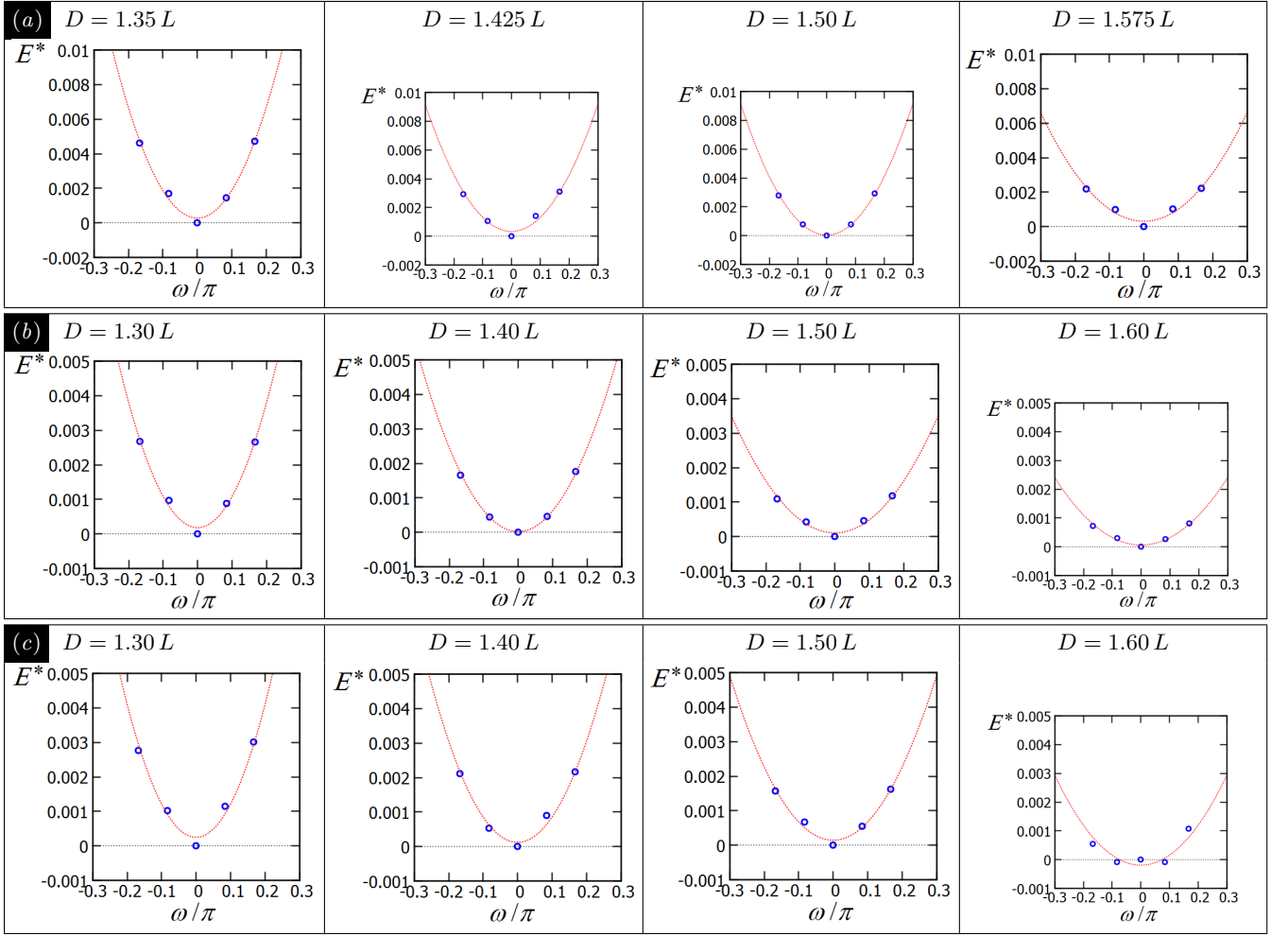


Figure S12: Energy  $E_N(\omega, \eta)$ , obtained through our numerical method and in units of  $\Sigma \gamma$  (with  $\gamma$  the fluid-fluid surface tension and  $\Sigma$  the particle surface area), for highly truncated-edge cubic particles at a fluid-fluid interface and in the lattice phase (a)  $x$ , (b)  $h$ , and (c)  $s$ , where  $\omega$  is the out-of-equilibrium azimuthal rotation we impose on one particle (for the exact definition of the particle configuration used here for each phase see Fig. 12). The blue symbols are  $E^* \equiv [E_N(\omega, \eta) - E_N(\omega = 0, \eta)]/(\Sigma \gamma)$  obtained for various particle-particle center-of-mass distances  $D$ , corresponding to different particle densities  $\eta$  (see Appendix C, Sec. B). The red dotted lines represent a fit of  $E_N(\omega, \eta) - E_N(\omega = 0, \eta)$  with  $U(\omega) \equiv C(\eta) \frac{\omega^2}{2}$ . The values of  $C(\eta)$  obtained from the fit for the various phases are shown in Fig. 12.